Chapter 1

Introduction

1.1 CO_2 in the global carbon cycle

Carbon dioxide (CO_2) is the most important anthropogenic greenhouse gas in the earth's atmosphere. Over the past half-century, atmospheric CO_2 concentrations have increased at a rate that correlates with the increase in anthropogenic fossil fuel burning and deforestation [*Solomon et al.*, 2007]. Carbon budget inventories indicate, however, that not all of the CO_2 released into the atmosphere from these activities persists in the atmosphere; approximately half of the anthropogenic CO_2 flux is sequestered in the oceanic and land biospheres [*Ciais et al.*, 1995]. Modeling the fate of anthropogenic CO_2 becomes a considerable technical challenge because of myriad interactions between the atmosphere, the oceans, and the terrestrial biosphere. Our ability to predict future changes in the carbon cycle and their effects on global climate relies on our quantitative understanding of these interactions.

The first step towards understanding these interactions is learning how to differentiate between atmospheric CO_2 molecules derived from various sources and sinks, so we can eventually de-convolve atmospheric observations into their individual components and describe the workings of the global budget through those observations. This task is more complex than it might at first seem because the atmosphere mixes efficiently over the atmospheric lifetime of CO_2; thus each parcel of air contains CO_2 molecules with many different origins and fates (see Figure 1.1). We find some of the needed constraints for these interactions in the variations of naturally occurring stable isotopes.

1.2 Stable isotopes, 'clumped' and otherwise

The stable isotope composition of CO_2 (i.e., the relative abundances of those isotopes that do not decay radioactively: ^{12}C, ^{13}C, ^{16}O, ^{17}O and ^{18}O) varies according to its sources and subsequent atmospheric chemistry and transport. Physical, chemical kinetic, and equilibrium isotope effects act together to determine the stable isotope composition of CO_2 in a given parcel of air. Differences in mass and symmetry of the twelve distinct CO_2 isotopologues (isotopic variants, e.g., $^{12}C^{16}O_2$, $^{13}C^{16}O_2$, $^{16}O^{12}C^{18}O$, $^{16}O^{13}C^{17}O$, etc.) formed from the five stable isotopes lead to subtle, but measurable differences in the rate of chemical transformations such as photosynthesis, respiration, air-sea exchange, or photochemical reactions.

In principle, measuring the stable isotope distribution in CO_2 could lead to an exceptionally detailed analysis of the 'history' of CO_2 in every sample of the atmosphere, as each natural process imparts its own unique isotopic signature; however, only four of these twelve isotopologues ($^{12}C^{16}O_2$, $^{13}C^{16}O_2$, $^{16}O^{12}C^{17}O$, and $^{16}O^{12}C^{18}O$) have been used extensively as tracers in atmospheric chemistry. By themselves, they are insufficient to constrain the relative influences of all the sources and sinks that have acted on a single sample. The remaining eight species (all of which contain two or three heavy rare isotopes) are exceptionally rare and, until recently, were considered to be essentially un-analyzable in natural materials. Measuring these very rare 'clumped' isotopologues would add new and essential independent constraints on the origins of CO_2 in samples of air.

In the laboratory, an equally daunting challenge exists: What are the most important reactions governing the isotopic composition of atmospheric CO_2, and what are the fundamental isotope effects? We wish to know, in the end, if our knowledge of the pertinent atmospheric chemistry is sufficient to explain atmospheric observations.

1.3 Anomalous isotopic enrichments in stratospheric CO_2

Shortly after the discovery of 'mass-independent' enrichments of ^{18}O and ^{17}O in stratospheric ozone [*Mauersberger*, 1981, 1987] and the demonstration of its chemical origin

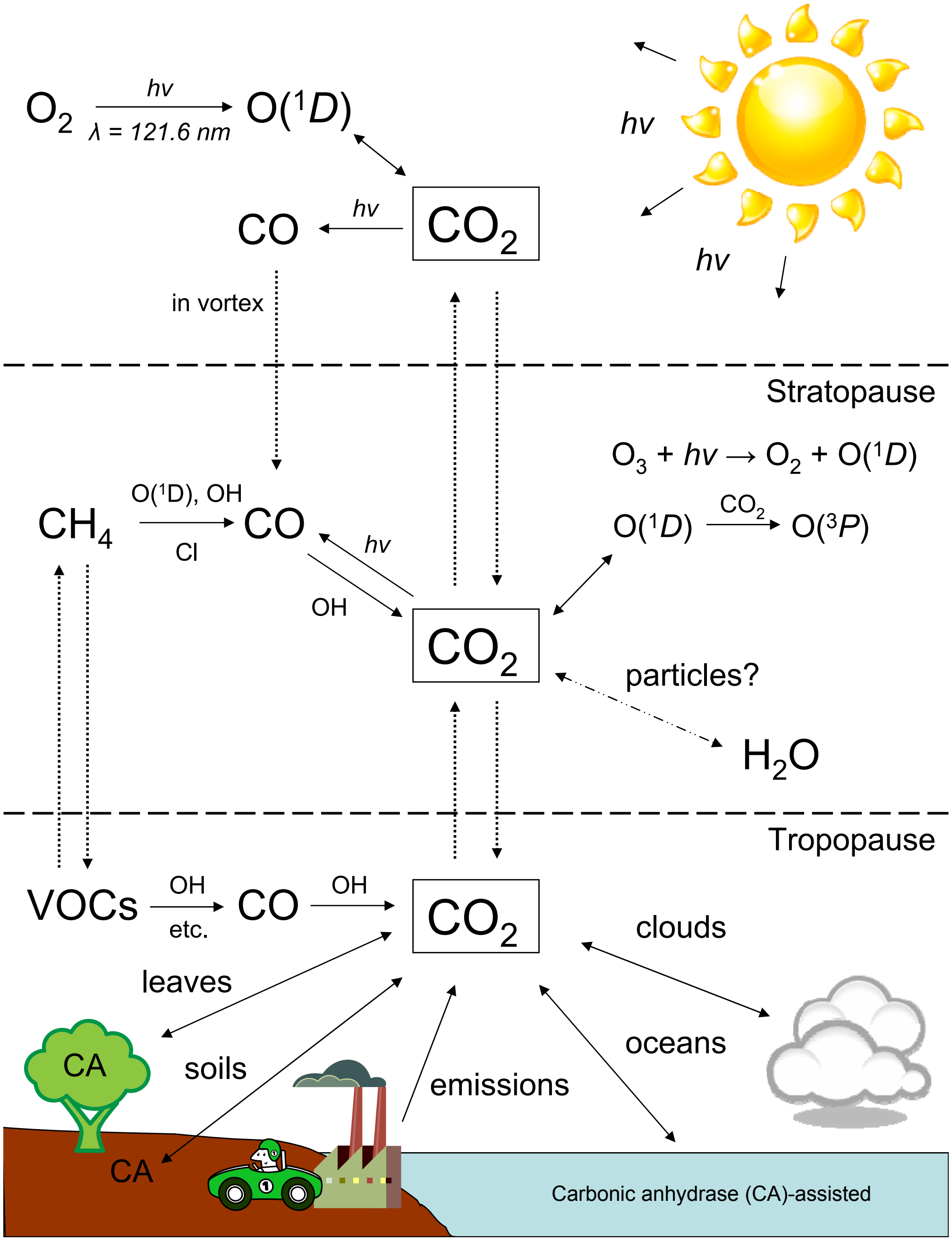

Figure 1.1: **Schematic of atmospheric CO_2 sources and sinks.** Photochemical reactions (single-headed arrows), isotope exchange reactions (double-headed arrows), and atmospheric transport (dotted arrows) are shown. Isotopic exchange on stratospheric liquid water and/or acid particles is uncertain, so its double-headed arrow is dashed.

[*Thiemens and Heidenreich*, 1983], similar enrichments were observed in stratospheric CO_2 (e.g., Figure 1.2) [*Alexander et al.*, 2001; *Boering et al.*, 2004; *Gamo et al.*, 1989; *Kawagucci et al.*, 2008; *Lämmerzahl et al.*, 2002; *Thiemens et al.*, 1991, 1995]. *Yung et al.* [1991] suggested that photochemical transfer of the heavy-isotope signature ($\Delta^{17}O$) from O_3 to CO_2 stratospheric CO_2 was possible after photolysis of O_3:

$$\mathrm{O_3} + h\nu(\lambda < 305\ \mathrm{nm}) \rightarrow \mathrm{O_2} + \mathrm{O}(^1D) \tag{1.1}$$

$$\rightarrow \mathrm{O_2} + \mathrm{O}(^3P) \tag{1.2}$$

and then subsequent isotope exchange through reaction 1.3:

$$\mathbf{O}(^1D) + \mathrm{CO_2} \rightarrow \mathbf{O}\mathrm{CO}_2^* \rightarrow \mathrm{O}(^3P) + \mathbf{O}\mathrm{CO} \tag{1.3}$$

The authors cited the isotope exchange mechanism in Baulch and Breckenridge's early study of the reaction in which the incident oxygen atom was incorporated into the product CO_2 molecule 2/3 of the time [*Baulch and Breckenridge*, 1966]. While this 'statistical' mechanism could explain the stratospheric ^{18}O and ^{17}O measurements qualitatively, a quantitative discrepancy remained between the observed and modeled $^{17}O/^{16}O$ vs. $^{18}O/^{16}O$ relationships: ^{17}O in CO_2 was more enriched than reaction 1.3 and Yung's model would have predicted. Unfortunately, the isotope effects in O_3 formation and photolysis and in the $O(^1D) + CO_2$ isotope exchange reaction (reaction 1.3) were not yet well understood.

Tests of the 'statistical' isotope exchange hypothesis were first conducted by *Wen and Thiemens* [1993], who photolyzed a mixture of O_3 and CO_2 with a mercury lamp at 254 nm. They observed heavy-atom enrichments in CO_2 that implied a non-statistical isotope exchange mechanism between O_3 and CO_2 (i.e., ^{17}O appeared to be preferentially incorporated into CO_2), but their result was misleading; the isotopic composition of the incident $O(^1D)$ changed significantly over the course of their experiment due to $O(^3P)$ and O_2 recombination. They did not account for these effects and thus were led to a spurious conclusion, as a later study showed [*Johnston et al.*, 2000]. To date, only one of these bulk photochemical experiments has been able to reproduce the relative ^{17}O-to-^{18}O enrichments observed in

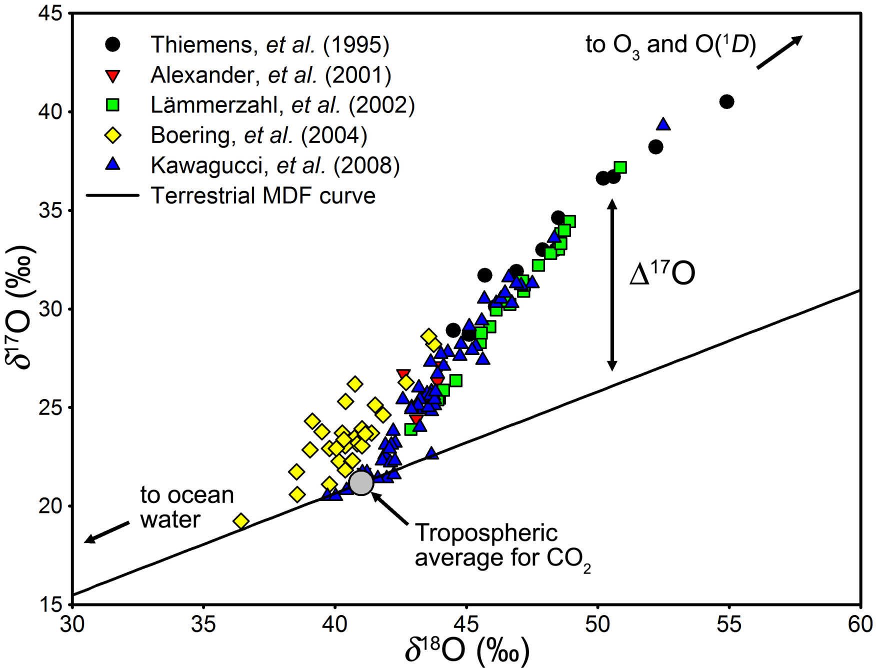

Figure 1.2: **Bulk oxygen isotope composition of stratospheric CO_2.** Departure from 'mass-dependent' compositions ($\Delta^{17}O$; see Appendix 1.A) are observed, owing to oxygen isotope exchange with stratospheric O_3 through reaction 1.3.

the stratosphere [*Chakraborty and Bhattacharya*, 2003], and those results have been controversial [*Shaheen et al.*, 2007]. Mechanistic insights have been limited because bulk stable isotope analysis is not able to differentiate isotope effects in O_3 photolysis and formation from isotope effects in reaction 1.3 unambiguously. Recent theoretical and modeling work on ozone has shed light on the effects of the former [*Babikov et al.*, 2003; *Cole and Boering*, 2006; *Gao and Marcus*, 2001, 2002; *Gao et al.*, 2002; *Hathorn and Marcus*, 1999, 2000; *Schinke et al.*, 2006], but the understanding of the stratospheric CO_2 isotopic distribution remains incomplete. The persistence of this field-laboratory disagreement was the primary inspiration for the 'clumped' isotope studies of reaction 1.3 described in this dissertation.

1.4 Insights from the physical chemist's toolbox

The techniques of physical chemistry have been invaluable for unraveling features in the complex mechanism of reaction 1.3. CO_3^* was believed to play a critical role in the isotope exchange reaction ever since the first experiments of *Katakis and Taube* [1962].

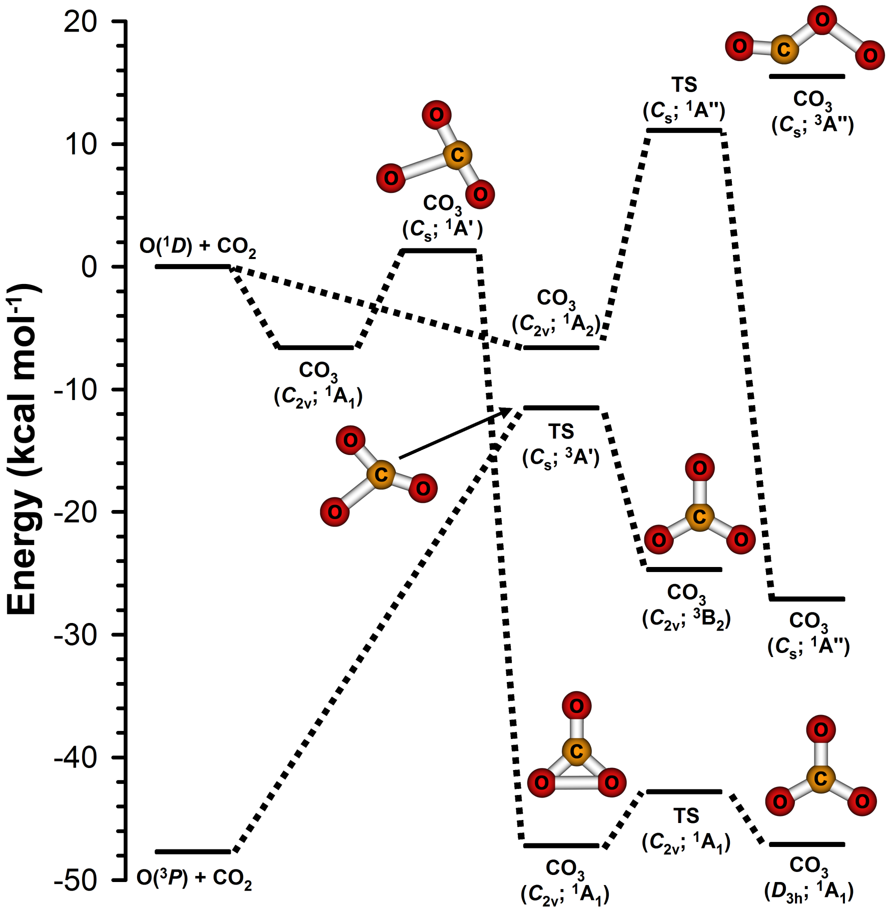

Figure 1.3: **Potential energy surface for $CO_3(^3A'')$ from *Mebel et al.* [2004].** Geometries were optimized at the CASSCF(16,13)/6-311G(d) level of theory. Energies were calculated at the MRCI+Q(16,13)/6-311+G(3df) level of theory.

Moll et al. [1966] first identified a CO_3 molecule spectroscopically upon irradiating CO_2 ice with vacuum-UV light. Although their data implied that stable CO_3 had C_{2v} symmetry, their experiments with ^{18}O-labeled CO_2 ices indicated that a $CO_3(D_{3h})$ species might be important in a reaction between atomic oxygen and CO_2, as was implied by the statistical mechanism of *Baulch and Breckenridge* [1966].

The $O(^1D) + CO_2$ potential energy surface (PES) calculated by *Mebel et al.* [2004] is shown in Figure 1.3. On the $^1A_1$ surface ($^1A'$ dynamically), the association reaction has an early barrier at 1 kcal mol^{-1}, which is consistent with its collision-limited reaction rate coefficient (1×10^{-10} cm^3 $molecule^{-1}$ s^{-1}) [*Sander et al.*, 2006]. The binding energy of $CO_3(^1A_1)$ is nearly 50 kcal mol^{-1}, and two structures (C_{2v} and D_{3h}) were predicted as bound species at the bottom of the potential well. $CO_3(C_{2v})$ was detected shortly thereafter in a low-temperature CO_2 matrix [*Bennett et al.*, 2004]; the presence of a true $CO_3(D_{3h})$ minimum on the PES had been debated (see *Kaiser and Mebel* [2008]; *Kowalczyk and Krylov* [2007]; *Liu et al.* [2009] and references therein), but it was recently detected experimentally in a 10 K CO_2 ice bombarded with high-energy electrons [*Jamieson et al.*, 2006].

Intersystem crossing (ISC) from the singlet to the triplet PESs is believed to occur through nonradiative transitions rather than through the minimum of the intersection seam (near the $^3A'$ transition state); the product $O(^3P_j)$ spin-orbit state distribution is consistent with an adiabatic CO_3 dissociation [*Matsumi et al.*, 1994a]. The ISC rate was also calculated to be ten times faster through a radiationless transition than through the singlet-triplet crossing seam [*Mebel et al.*, 2004]. *Yang et al.* [2005] later proposed that a direct quenching mechanism (i.e., not through a CO_3 complex) might also be important.

Gas-phase studies of reaction 1.3 show evidence for CO_3, though none have detected it directly. *Perri et al.* [2003, 2004] reported evidence for a long-lived $CO_3{}^*$ reaction complex in their crossed-molecular-beam experiments. This long-lived (1 – 10 ps lifetime) intermediate had been suggested in previous temperature- and pressure-dependent studies [*Clerc and Reiffsteck*, 1968; *DeMore and Dede*, 1970; *Weissberger et al.*, 1967], but never directly confirmed; its lifetime was later confirmed to be long enough for nearly statistical intramolecular vibrational redistribution [*Chen et al.*, 2009]. The structure and dynamics of CO_3 are not yet completely understood, however. For instance, $O(^1D)$ + CO_2 collision energy appears to be important dynamically; *Perri et al.* [2003, 2004] reported that $O(^1D)$ + CO_2 collisions yielded spin-conserving, isotopically exchanged products (1.4):

$$\mathbf{O}(^1D) + CO_2 \rightarrow \mathbf{O}CO_2^* \rightarrow O(^1D) + \mathbf{O}CO \tag{1.4}$$

Their crossed-molecular-beam experiments were performed at elevated collision energies (4.2 and 7.7 kcal mol^{-1}) so the importance of reaction 1.4 to the stratosphere is unknown. *Mebel et al.*'s companion computation study suggested that reaction 1.4 has a ~5% branching fraction at stratospheric collision energies, but this prediction has not been tested. Still, *Perri et al.*'s experimental result casts significant doubt on the applicability of the previous bulk photochemical experiments. All the recent studies of the $O_2/O_3/CO_2$ photochemical system used O_2/O_3 as a source of $O(^1D)$ with a significant mixing fraction of CO_2, so the $O(^1D)$ atoms reacting with CO_2 probably had an elevated average kinetic energy as high as ~9 kcal mol^{-1} [*Thelen et al.*, 1995], six times the calculated average in the stratosphere [*Kharchenko and Dalgarno*, 2004; *Takahashi et al.*, 2002].

1.5 Executive summary

This dissertation describes studies of three oxygen isotope exchange reactions involving CO_2 — one well-studied and two we discovered — and their potential implications for oxygen cycling in the upper atmosphere. First, I will describe the meridional (latitudinal) variations of stratospheric $^{16}O^{13}C^{18}O$ relative to those of $^{12}C^{16}O_2$, $^{13}C^{16}O_2$, $^{16}O^{12}C^{18}O$, and $^{16}O^{12}C^{17}O$; we identified a meridional gradient, with $^{16}O^{13}C^{18}O$ most enriched at the Arctic polar vortex. Our experimental and modeling study revealed that the variations in $^{16}O^{13}C^{18}O$ proportions cannot be explained in full by the known stratospheric chemistry affecting CO_2. Instead, we propose — because of the localization of a $^{16}O^{13}C^{18}O$ anomaly in the wintertime pole — that the chemistry either in the mesosphere or on stratospheric particles leads to the newly discovered isotopic enrichments. Second, I will describe crossed-molecular-beam experiments that led to the discovery of the isotope exchange reaction O_2 + CO_2. We show that the isotope exchange reaction occurs through a short-lived CO_4 intermediate, and that an adiabatic reaction mechanism exists despite a variety of energetically accessible product channels. Third, I will discuss a computational and laboratory dynamics study of hyperthermal collisions between ground-state oxygen-atoms and CO_2. We identified two reactions: oxygen-atom isotope exchange and abstraction. The isotope exchange reaction proceeds through a short-lived CO_3^* reaction complex, and it may have implications for the oxygen-isotope budget in the upper atmosphere and/or the stratospheric polar vortex. The oxygen-atom abstraction reaction may proceed through either a ‘stripping’-type mechanism or a CO_3 complex, although the data cannot distinguish between the two mechanisms definitively. In the final chapter, I will attempt to synthesize what we have learned from these three studies, and what questions have emerged as a result.

Appendices

1.A Isotopic notation

The natural abundance of the rare isotopes that are the focus of this thesis are 1.1% (^{13}C), 0.02% (^{18}O), and 0.038% (^{17}O). Variations in these stable isotope abundances are typically $\leq 10^{-3}$. Consequently, bulk stable isotope abundances are commonly reported in δ-notation, in units of per mil (‰):

$$\delta^{13}\mathrm{C} = \left(\frac{R^{13}_{\mathrm{sample}}}{R^{13}_{\mathrm{VPDB}}} - 1 \right) \times 1000 \tag{1.5}$$

$$\delta^{18}\mathrm{O} = \left(\frac{R^{18}_{\mathrm{sample}}}{R^{18}_{\mathrm{VSMOW}}} - 1 \right) \times 1000 \tag{1.6}$$

where R^n is the abundance ratio of a rare isotope or isotopologue of mass n to its most abundant analogue, i.e.,

$$R^{13} = \frac{[^{13}\mathrm{C}]}{[^{12}\mathrm{C}]} \qquad R^{18} = \frac{[^{18}\mathrm{O}]}{[^{16}\mathrm{O}]} \qquad R^{17} = \frac{[^{17}\mathrm{O}]}{[^{16}\mathrm{O}]} \tag{1.7}$$

$\delta^{17}O$ is defined similarly to $\delta^{18}O$ in Eq. 1.6. $\delta^{13}C$, $\delta^{18}O$, and $\delta^{17}O$ are reported relative to the international standards VPDB (Vienna Pee Dee Belemnite; $R^{13} = 0.0112372$) and VSMOW (Vienna Standard Mean Ocean Water; $R^{18} = 0.0020052$ and $R^{17} = 0.0003799$). These standards were established under the International Atomic Energy Agency, but are otherwise arbitrary. They represent convenient reference points against which all isotopic measurements can be compared. Positive δ-values mean that the sample bulk isotope composition is enriched relative to the standard, and negative δ-values mean that the sample bulk isotope composition is depleted relative to the standard.

Within bulk stable isotope geochemistry, a second family of notation has emerged since the discovery of 'mass-independent' oxygen isotope fractionation (MIF) in carbonaceous chondrites [*Clayton et al.*, 1973] and during the formation of ozone (O_3) [*Thiemens and Heidenreich*, 1983]. The magnitude of MIF in oxygen ($\Delta^{17}O$) is defined in Eq. 1.8:

$$\Delta^{17}\mathrm{O} = \delta^{17}\mathrm{O} - 0.516 \times \delta^{18}\mathrm{O} \tag{1.8}$$

This terminology is used to describe deviations from the canonical mass-dependent isotopic relationships derived by *Urey* [1947] and Bigeleisen [*Bigeleisen and Mayer*, 1947; *Bigeleisen and Wolfsberg*, 1958]. Most equilibrium and kinetic isotope effects are half as pronounced for $^{17}O/^{16}O$ ratios vs. $^{18}O/^{16}O$ ratios, so the slope of a $\delta^{17}O$ vs. $\delta^{18}O$ plot (similar to $^{17}O/^{16}O$ vs. $^{18}O/^{16}O$) is nominally 0.5. Departures from mass-dependent fractionation in oxygen are calculated using Eq. 1.8: $\Delta^{17}O > 0$ represents a 'mass-independent' enrichment in ^{17}O, whereas $\Delta^{17}O < 0$ represents a "mass-independent" depletion in ^{17}O. Several excellent reviews of this topic have been published, e.g., *Weston* [1999] and *Thiemens* [2006].

The language of 'clumped' isotope geochemistry is potentially even more confusing because the reference isotopic ratio (e.g., the denominator in Eq. 1.6) is no longer a constant:

$$R^{47} = \frac{[^{47}CO_2]}{[^{44}CO_2]} \qquad \Delta_{47} = \left(\frac{R^{47}_{\text{sample}}}{R^{47}_{\text{stochastic}}}) - 1\right) \times 1000 \tag{1.9}$$

In Eq. 1.9, $R^{47}_{\text{stochastic}} = 2R^{13}R^{18} + 2R^{17}R^{18} + R^{13}(R^{17})^2$, the distribution of stable carbon and oxygen isotopes if they were randomly distributed among all isotopologues of CO_2 [*Eiler*, 2007]. It is important to recognize that the terms used in 'clumped' isotope geochemistry (Eq. 1.9) differ fundamentally from those in bulk-isotope measurements; the "reference" to which the measured R^{47}_{sample} is compared is a *varying internal* standard (the bulk isotopic composition), rather than the *fixed external* standard used in Eqs. 1.5 and 1.6. This distinction also leads to quirky, yet ultimately useful changes in Δ_{47} when subject to various physical processes such as mixing and diffusion [*Eiler and Schauble*, 2004].

A common question has been: "What is the difference between an isotopo*mer* and an isotopo*logue*?" Two isotopo*mers*, like chemical isomers, share the same isotopic composition, but the stable isotopes themselves are in positions that render the two molecules chemically distinct. A good example can be found in the comparison of isotopically substituted N_2O and CO_2 molecules: $^{14}N–^{15}N–^{16}O$ and $^{15}N–^{14}N–^{16}O$ are isotopo*mers* of one another because the N-atom substitutions are not symmetrically equivalent. The two isotopomers, consequently, have differing chemical properties, e.g., vibrational frequencies and rotational constants. In contrast, $^{16}O–^{12}C–^{18}O$ and $^{18}O–^{12}C–^{16}O$ are equivalent upon rotation, so they are equivalent structures of a single isotopo*logue*.

1.B Copyright declaration

This thesis contains excerpts from three publications in which the author was involved:

- Huntington, K. W., J. M. Eiler, H. P. Affek, W. Guo, M. Bonafacie, L. Y. Yeung, N. Thiagarajan, B. Passey, A. Tripati, M. Daëron, R. Came (2009), Methods and limitations of 'clumped' CO_2 isotope (Δ_{47}) analysis by gas source isotope ratio mass spectrometry, *J. Mass Spectrom.*, *44*(9), 1318–1329. ©2009 John Wiley & Sons.

- Yeung, L. Y., H. P. Affek, K. J. Hoag, W. Guo, A. A. Wiegel, E. L. Atlas, S. M. Schauffler, M. Okumura, K. A. Boering, and J. M. Eiler (2009), Large and unexpected enrichment in stratospheric $^{16}O^{13}C^{18}O$ and its meridional variation, *Proc. Natl. Acad. Sci. U. S. A.*, *106*(28), 11,496–11,501. ©2009 National Academy of Sciences.

- Yeung, L. Y., M. Okumura, J. T. Paci, G. C. Schatz, J. Zhang, and T. K. Minton (2009), Hyperthermal O-Atom Exchange Reaction O_2 + CO_2 through a CO_4 Intermediate, *J. Am. Chem. Soc.*, *131*(39): 13,940–13,942. ©2009 American Chemical Society Publications.